Reports

Detection of C_3 in the Circumstellar Shell of IRC+10216

KENNETH W. HINKLE, JOHN J. KEADY, PETER F. BERNATH

Vibration-rotation lines of C_3 have been identified in the circumstellar spectrum of the obscured carbon star IRC+10216. This molecule is of interest in both the chemistry of flames, where it may be involved in the formation of soot, and in astrophysics, where it is a potential building block for carbonaceous grains. This high-resolution infrared detection of the pure carbon chain molecule C_3 allows the estimation of the equilibrium C–C bond length, 1.297 angstroms. Possible astrophysical formation and destruction mechanisms for C_3 are reviewed, including the relationship between C_3 and carbon clusters.

A UNIQUE GROUP OF SPECTRAL lines at 4050 Å was first detected in the spectrum of a comet in 1881 (1). It was not until 1951 that A. E. Douglas (2) was able to attribute the 4050 Å group to the C_3 molecule. The most thorough analysis of the $\tilde{A}^1\Pi_u$–$\tilde{X}^1\Sigma_g^+$ transition of C_3 was carried out by Gausset, Herzberg, Lagerquist, and Rosen (3). In addition to comets and electrical discharges, the C_3 molecule has been observed in flames (4) and explosions (5) and in the vaporization of carbon (6). There is some low-resolution evidence for the appearance of C_3 in the atmospheres of cool stars (7). In flames, C_3 may be a critical link in the formation of soot (4). In astrochemistry, pure carbon chains, including C_3, have been linked to the formation of circumstellar grains (8) and may be involved in the formation of diffuse interstellar bands (9).

The detection of C_3 in carbon stars and in the interstellar medium is inhibited by lack of ultraviolet (UV) flux at 4050 Å. Because C_3 is linear (3) or quasilinear (10) there is neither a dipole moment nor strong microwave pure rotational transitions. There are three vibrational modes, ν_1 the symmetric stretch (σ_g^+) at 1224.5 cm^{-1} (11), ν_2 the bending mode (π_u) at 63.1 cm^{-1} (3), and ν_3 the antisymmetric stretch (σ_u^+) at 2040 cm^{-1} (12). However, ν_1 is Raman active, not infrared active, and ν_2 occurs in the far infrared, which remains a difficult spectral region to observe. The antisymmetric stretch, ν_3, is ideal for monitoring C_3 because it has a remarkably strong transition dipole moment of 0.44 D (10) and occurs in

K. H. Hinkle, Kitt Peak National Observatory, National Optical Astronomy Observatories, Tucson, AZ 85726.
J. J. Keady, Theoretical Division, Los Alamos National Laboratory, Los Alamos, NM 87545.
P. F. Bernath, Department of Chemistry, University of Arizona, Tucson, AZ 85721.

a spectral region where the atmosphere is relatively transparent.
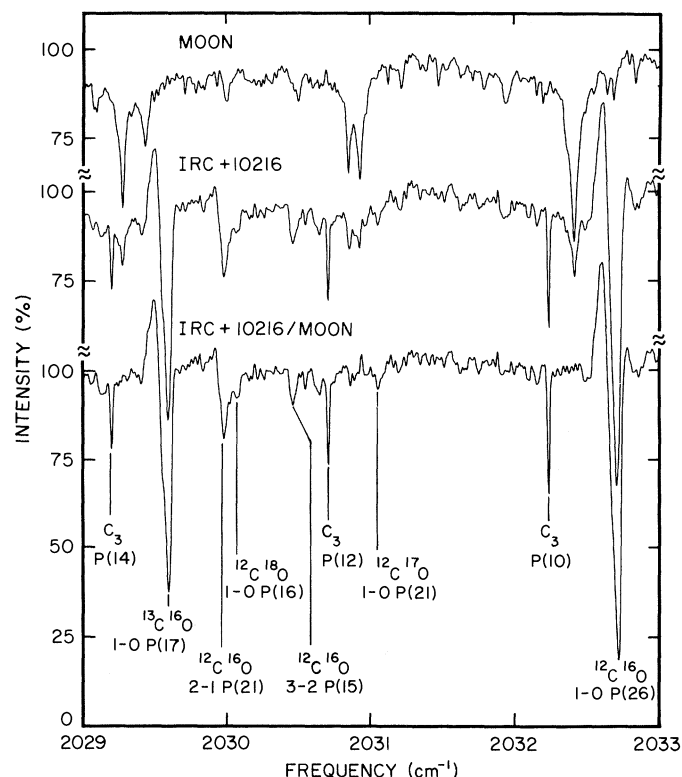
On 30 December 1987 spectra of the prototypical obscured carbon star IRC+10216 and the moon were observed with an apodized (13) resolution of 0.014 cm^{-1} (2 km s^{-1} full width at half maximum) by means of the Kitt Peak National Observatory 4-m telescope and the Fourier Transform spectrometer located at the coudé focus (14). The 52-min integration on IRC+10216 resulted in a peak signal-to-noise (1 sigma) ratio of 112. The spectrum was limited to 1975 to 2050 cm^{-1} by a cold

Fig. 1. A short section of the spectrum of the moon, IRC+10216, and the ratio IRC+10216/moon showing three of the C_3 lines. Also identified are CO lines of various isotopic species. The CO lines are formed throughout the circumstellar shell and have a different line shape and excitation temperature from the C_3. The moon, which serves as a reference for the telluric spectrum, was observed at a larger air mass than IRC+10216 and hence the telluric spectrum is stronger. The air mass difference between IRC+10216 and the moon has been adjusted in the ratio. The frequency scale has not been corrected for the earth's velocity. See text to convert the C_3 frequencies to laboratory values.

blocking filter. The moon is an intrinsically featureless source in the 2000 cm^{-1} region. After appropriately scaling the telluric line strengths to match the air mass of the IRC+10216 spectrum, the lunar spectrum was ratioed to the IRC+10216 spectrum to remove the telluric spectrum.

The goal of our observations was to detect the CN vibration-rotation fundamental (15). IRC+10216 is frequently used for high sensitivity searches of circumstellar molecules because it is a bright source and lines of circumstellar origin appear against a featureless continuum, not superposed on photospheric lines (16). Although the CN lines were not obviously present (17), a series of strong lines was observed (Fig. 1), which on the basis of combination differences (3) were identified as C_3. More R branch lines were identified on an archival spectrum (18 October 1978, resolution 0.026 cm^{-1}, S/N = 95) that covered the 2040 to 2170 cm^{-1} region. Prior to the discovery reported in this paper of the C_3 ν_3 band in the circumstellar envelope of the carbon star IRC+10216, no high resolution spectroscopic observations of the infrared spectrum of C_3 were available.

At the time this work was completed no laboratory frequencies were available for the 2040 cm^{-1} C_3 lines, thus the frequencies had to be derived from our spectrum. To do this we assumed that, in analogy to the other molecules observed in the infrared with similar line shape and excitation temperature

(see below), the lines exist in the circumstellar shell at the terminal expansion velocity, -14 km s^{-1} relative to the center of mass (16). Assuming this velocity and correcting for a local standard of rest velocity of -26 km s^{-1} for IRC+10216 (18) and for the earth's velocity at the time of the observation, frequencies were measured. Telluric CO_2 lines (19) gave the frequency zero point. Subsequent to the submission of this report, we have learned of two research groups reporting laboratory detections of the ν_3 band of C_3 (20). The laboratory observations agree with the work reported here.

The observed line positions (Table 1) were reduced to the molecular constants by means of the customary (21) rotational energy level expression:

$$F(J) = BJ(J + 1) - D[J(J + 1)]^2 \quad (1)$$

where B and D are constants, and J is the angular momentum quantum number. The constants obtained from this fit are reported in Table 2.

The high resolution detection of ν_3 completes the analysis of the C_3 fundamental modes of vibration and allows the derivation of an equilibrium molecular structure. The vibrational dependence of the rotational constants can be represented by (3, 11, 21)

$$B_{\nu_1\nu_2\nu_3} = 0.41767 - 0.0048\left(\nu_1 + \frac{1}{2}\right)$$

$$+ 0.01345(\nu_2 + 1) - 0.00071(\nu_2 + 1)^2$$

$$+ 0.00510\left(\nu_3 + \frac{1}{2}\right) \quad (2)$$

where ν_i is the vibrational quantum number of mode ν_i. From the value of B_e, 0.41767 cm^{-1}, the equilibrium C–C bond length (r_e) of 1.2968 Å was calculated. The total error in r_e is hard to assess because the extremely floppy C_3 molecule executes large-amplitude bending motions (10), but ± 0.001 Å seems a reasonable assumption. The equilibrium bond length of a molecule is an easy quantity to compute by ab initio quantum chemical calculations. For example, Kraemer, Bunker, and Yoshimine (10) obtain 1.290 Å, whereas Peric-Radic et al. (22) obtain 1.308 Å, both in good agreement with experiment. The r_0 value calculated from $B_{000} = 0.43056$ cm^{-1} (Table 2) is 1.277 Å, rather different from the r_e value because of the large-amplitude vibrational motion.

One unusual feature of the ν_3 mode is the vibrational dependence of the rotational constant $B_{\nu_1\nu_2\nu_3}$. For most linear molecules the rotational constants of the antisymmetric stretching mode decrease with increasing vibrational excitation but for C_3 the opposite trend is observed. The nonrigid bender calculations of Kraemer, Bunker, and Yoshi-

mine (10) predict this effect; α_3 (calculated) $= -0.003$ cm^{-1} compared to α_3 (observed, this work) $= -0.00510$ cm^{-1}.

The C_3 lines in the spectrum of IRC+10216 appear to be saturated and we have used an observer's frame radiative transfer code to model the lines in the circumstellar shell (23). Lacking a detailed knowledge of the spatial distribution, we assume a r^{-2} density distribution truncated at some inner radius. The assumption of a continuous C_3 distribution throughout the envelope, as if the C_3 originated in the photosphere similar to CO, C_2H_2, HCN, and CS (16, 23–25), results in synthesized line profiles that bear no resemblance to the observations. The line profiles of species with continuous distributions are strongly influenced by higher temperature ($T > 100$ K) gas in the inner regions (26) ($r < 300$ R_*, where 1 $R_* = 6.7 \times 10^{13}$ cm) of the circumstellar shell (23). Moreover, the $(0,1,1) \leftarrow (0,1,0)$ "hot" band, whose lower level lies only 63 cm^{-1} above the ground state, falls within our bandpass. It is not seen. For a continuous distribution of C_3, the model's warm gas results in synthetic hot band line strengths that start to rival the cold band line strengths.

The observed rotational distribution of C_3 is inconsistent with a photospheric origin and widespread distribution similar to that of the molecules discussed above. Given the

Table 1. C_3 lines observed in the 4.9-μm spectrum of IRC+10216.

Line	Frequency* (cm^{-1})	Equivalent width (mK)	Comment
P(18)	2025.877:	1.5	
P(16)	2027.345	1.6	
P(14)	2028.824	4.3	
P(12)	2030.327	5.2	
P(10)	2031.855	6.6	
P(8)	...	...	Telluric line
P(6)	2035.006	9.3	
P(4)	2036.637	8.8	
P(2)	2038.308	6.1	
R(0)	...	...	Telluric line
R(2)	2042.665	8.0	
R(4)	2044.478	9.8	
R(6)	2046.325:	8.:	In wing of telluric line
R(8)	2048.206	11.7	Poor S/N in 1987 spectrum†
R(10)	...	...	Telluric line
R(12)	2052.046	8.2	
R(14)	2053.995:	9.3	Blend
R(16)	2055.957:	3.8	Blend

*The frequencies result from forcing the line to be at an expansion velocity of 14 km s^{-1} in the circumstellar shell. †R(2), R(4), R(6), and R(8) have been measured in both spectra and the frequencies agree to 1×10^{-3} cm^{-1}. The colons indicate values with larger uncertainties.

small rotational constant of ~ 0.43 cm^{-1}, the significant strength in the low J lines (unresolved and $\sim 50\%$ deep) and the apparent lack of absorption for lines with $J > 20$ imply that the C_3 absorption arises well away from the photosphere. Using the undetected high excitation ($J > 20$) lines, we establish an upper limit on $x(C_3)$ of 1.5×10^{-7} in the warm, inner envelope (<300 R_*). With the assumption of an inner boundary at 350 R_*, the radiation transport calculations require a range of temperature, from 70 K to ~ 20 K, and a C_3 column density of $1(\pm 0.15) \times 10^{15}$ cm^{-2}. The strongest C_3 lines have optical depths of about unity. The fractional abundance of C_3 relative to molecular hydrogen, $x(C_3)$, is 1.2×10^{-6} in the region modeled. The strongest synthesized lines in the $(0,1,1) \leftarrow (0,1,0)$ hot band are $\sim 2\%$ deep, and are undetectable in our present spectrum. Higher signal-to-noise data will be very useful in further constraining the gas temperature. If the actual density distributions were more compact or peaked, then maintaining the same column density would require a larger fractional abundance. However, the range of temperature indicated by the transport calculations points toward an extended distribution.

The question arises as to the origin of the C_3. The difficulty with a direct photolysis origin for C_3 is the paucity of possible parent molecules. Methyl acetylene and its isomer allene, C_3H_4, are suspected C_3 photolysis parents in comets (27). It seems unlikely that such heavy molecules would be abundant enough in IRC+10216 (28) to account for the observed C_3 and, indeed, this seems to be the case. Upper limits of 3×10^{-7} have been found for the abundance of methyl acetylene (29), 2×10^{-7} for allene (25), and 5×10^{-7} for diacetylene (C_4H_2) (25). The cyanoacetylene (HC$_3$N) abundance is a few times 10^{-7} (30), subject to considerable uncertainty, making it difficult to rule out. However, laboratory studies of vacuum UV cyanoacetylene photolysis indicate the photodissociation daughters to be C_2H and CN (31).

In addition to direct photolysis, C_3 could be the result of photolysis and subsequent neutral or ion gas phase chemistry. Ion-molecule reaction schemes to form C_3, initiated by cosmic ray ionization of helium and (more importantly) acetylene photolysis have been suggested (32), but these manufacture C_3 only in the cold outer envelope ($r > 1000$ R_*, $T < 15$ K). The infrared (16) and microwave (33) C_2H observations are consistent with an outer envelope mother molecule abundance $x(C_2H_2) \sim 3 \times 10^{-6}$. With this assumption, our chemical kinetics and radiation transport calculations indicate

Table 2. Spectroscopic constants for the ν_3 vibrational mode of C_3.

Constant	Value (cm^{-1})
ν_3	2040.02113 (62)*
$B_{0,0,0}$	0.430557 (37)
$D_{0,0,0}$	1.415 (79) $\times 10^{-6}$
$B_{0,0,1}$	0.435654 (39)
$D_{0,0,1}$	3.937 (88) $\times 10^{-6}$

*One standard deviation uncertainty in parentheses. These errors are determined by the least-squares fit of the 15 line positions of Table 1.

that a few percent of the required amount of C_3 is formed. Even if the outer envelope acetylene abundance were an order of magnitude larger, the cold gas so produced could not account for the absorption in the higher excitation ($J > 6$) C_3 lines.

Carbon condensation products form another possible photolysis parent for C_3. Carbon condensation is thought to occur in or near the stellar photosphere (26) and may involve the growth of carbon clusters into macroscopic "grains" (8, 34). As nucleation effectively ceases, a remnant distribution of microscopic particles, C_n clusters, might survive. In laboratory experiments (8, 34), both clusters and macroscopic particles are produced subsequent to the laser vaporization of graphite. Still other experiments (35) suggest that single 3.5-eV photons are effective in fragmenting carbon cluster ions, and even suggest the existence (36) of a "magic" fragment, C_3. The intriguing possibility is that C_3 is but one photofragment daughter of a much larger carbon cluster, with other daughters (C_2, C_4, C_5, C_6, and so on) possible. Although the suggestion that the photolysis of carbon condensation products is a source of C_3 is attractive, the caveat must be made that none of the condensation products, except for grains, have been observed in the circumstellar envelopes of stars. Observational confirmation of these products in circumstellar envelopes will be difficult.

A possible problem with a hypothesized photolysis origin for C_3 is that species whose origin is known to be directly photolytic (C_2H and CN) occur much further out (16, 33) in the circumstellar shell at $r \sim 1000\ R_*$ and $T_{rot} \sim 12$ K. However, less energetic photons may be required to photofragment large carbon clusters than are required to fragment the photolysis parents of C_2H [$D(H-C_2H) = 5.4$ eV (31)] or CN [$D(H-CN) = 5.2$ eV (31)]. These less energetic photons penetrate the circumstellar envelope more deeply, because the dust is less opaque at the longer wavelengths. Thus C_3 could be photolytically produced and be warmer than the C_2H. Note that since C_3 lacks a permanent dipole moment, the radia-

tive and collisional excitation dynamics controlling the rotational temperature will differ from CN and C_2H (as well as SiO, CS, HCN, and SiS) in the sense of C_3 being potentially closer to local thermodynamic equilibrium, similar to the situation for other molecules having either no permanent dipole moment (CH_4, SiH_4, C_2H_2) or a small one (CO).

Of course, the C_3 could be formed on carbon-rich grains either through photolysis or, as is thought to be the case (25) for NH_3, CH_4, and SiH_4, catalytic reactions. With a standard model for the gas and dust density (26) and assuming a grain radius of 0.1 μm (16), and $x(C_3) \sim 10^{-6}$ at 400 R_*, we find that 10^5 carbon atoms must be released per grain. Although this is only 0.1% of the grain mass, this assumes all carbon atoms are released as C_3. Note the total relative abundance of the trace species NH_3, CH_4, and SiH_4 is $\sim 1 \times 10^{-6}$ (25), similar to the C_3 abundance. However, these presumably catalytically produced species seem to leave the grains in a considerably warmer region (25). This still leaves photolytic interactions with the grains as a possibility.

In addition to the origin of C_3, its subsequent chemical behavior is potentially of great importance to the chemistry of the circumstellar shell. Because H_2, C_2H_2, and HCN are highly abundant at $r < 100\ R_*$ in the circumstellar shell of IRC+10216 and because many complex hydrocarbons are observed at $r > 1000\ R_*$ (28), neutral gas phase reactions between H_2, C_2H_2, and HCN molecules, and C_3 are of potential importance. Studies (37) of ground-state C_3 reacting with other species indicate that the reaction rates are typically factors of 10^2 to 10^4 slower than the gas kinetic collision rate. If this relatively slow reactivity applies to the molecular collision partners likely to be encountered in the circumstellar envelope then, with the possible exception of molecular hydrogen (because of its large relative abundance), neutral gas phase reactions with C_3 probably are not important on the time scales involved. The C_3 bond energy is 7.3 eV (31) and the ionization potential is 12.1 eV (38). These large values imply a relatively long life for C_3 against the eventual photodestruction into the more reactive species C and C_2.

REFERENCES AND NOTES

1. W. Huggins, *Proc. R. Soc. London* **33**, 1 (1882).
2. A. E. Douglas, *Astrophys. J.* **114**, 446 (1951); K. Clusius and A. E. Douglas, *Can. J. Phys.* **32**, 319 (1954).
3. L. Gausset, G. Herzberg, A. Lagerquist, B. Rosen, *Astrophys. J.* **142**, 45 (1965).
4. A. G. Gaydon and H. G. Wolfhard, *Flames* (Chapman and Hall, London, 1978).
5. R. G. Norrish, G. Porter, B. A. Thrush, *Proc. R. Soc. London* **A216**, 165 (1953).

6. W. A. Chupka and M. G. Inghram, *J. Phys. Chem.* **59**, 100 (1955).
7. A. McKellar, *Astrophys. J.* **108**, 453 (1948); P. Swings, A. McKellar, K. N. Rao, *Mon. Not. R. Astron. Soc.* **113**, 571 (1953); D. Crampton, A. P. Cowley, R. M. Humphreys, *Astrophys. J.* **198**, L135 (1975); B. Zuckerman, D. P. Gilray, B. E. Turner, M. Morris, P. Palmer, *ibid.* **205**, L15 (1976).
8. H. W. Kroto, J. R. Heath, S. C. O'Brien, R. F. Curl, R. E. Smalley, *Astrophys. J.* **314**, 352 (1987).
9. R. E. S. Clegg and D. L. Lambert, *Mon. Not. R. Astron. Soc.* **201**, 723 (1982); see also A. E. Douglas, *Nature* **269**, 130 (1977).
10. W. P. Kraemer, P. R. Bunker, M. Yoshimine, *J. Mol. Spectrosc.* **107**, 191 (1984); see also R. Beardsworth, P. R. Bunker, P. Jensen, W. P. Kraemer, *ibid.* **118**, 50 (1986); P. Jensen and W. P. Kraemer, *ibid.* **129**, 172 (1988).
11. A. J. Merer, *Can. J. Phys.* **45**, 4103 (1967).
12. W. Weltner, P. N. Walsh, C. L. Angell, *J. Chem. Phys.* **40**, 1299 (1964).
13. R. H. Norton and R. Beer, *J. Opt. Soc. Am.* **66**, 259 (1976).
14. D. N. B. Hall, S. T. Ridgway, E. A. Bell, J. M. Yarborough, *Proc. Soc. Photo-Optical Instrum. Engineers* **172**, 121 (1978).
15. J. G. Phillips, *Astrophys. J.* **180**, 617 (1973); D. Cerny, R. Bacis, G. Guelachvili, F. Roux, *J. Mol. Spectrosc.* **73**, 154 (1978).
16. J. J. Keady and K. H. Hinkle, *Astrophys. J.* **331**, 539 (1988).
17. G. R. Wiedemann, D. E. Jennings, D. Deming, J. J. Keady, K. H. Hinkle, in preparation.
18. P. G. Wannier *et al.*, *Astrophys. J.* **230**, 149 (1979); H. Olofsson, L. E. B. Johansson, Å. Hjalmarson, Nguyen-Quang-Rieu, *Astron. Astrophys.* **107**, 128 (1982).
19. C. P. Rinsland *et al.*, *NASA Technical Memorandum 85764-Atlas of High Resolution Infrared Spectra of Carbon Dioxide: February 1984 Edition* (NASA, Washington, 1984).
20. K. Matsumura, H. Kanamori, K. Kawaguchi, E. Hirota, *J. Chem. Phys.*, in press; T. Amano, N. Moazzen-Ahmadi, A. R. W. McKellar, private communication.
21. G. Herzberg, *Electronic Spectra and Electronic Structure of Polyatomic Molecules* (Van Nostrand–Reinhold, New York, 1966).
22. J. Peric-Radic, J. Romelt, S. D. Peyerimhoff, R. J. Buenker, *Chem. Phys. Lett.* **50**, 344 (1977).
23. J. J. Keady, D. N. B. Hall, S. T. Ridgway, *Astrophys. J.* **326**, 832 (1988).
24. J. J. Keady, thesis, New Mexico State University (1982).
25. _____ and S. T. Ridgway, in preparation.
26. S. T. Ridgway and J. J. Keady, *Astrophys. J.* **326**, 847 (1988).
27. W. F. Huebner and P. T. Giguere, *ibid.* **238**, 753 (1980); W. F. Huebner, in *Photochemistry of Atmospheres*, J. S. Levine, Ed. (Academic Press, New York, 1985), pp. 437–481.
28. A. E. Glassgold and P. J. Huggins, in *NASA Special Publication 492, The M-Type Stars*, H. R. Johnson and F. R. Querci, Eds. (NASA, Washington, 1986), pp. 291–322.
29. L. E. B. Johansson *et al.*, *Astron. Astrophys.* **130**, 227 (1984).
30. J. H. Bieging and Nguyen-Quang-Rieu, *Astrophys. J.* **329**, L107 (1988).
31. H. Okabe, *Photochemistry of Small Molecules* (Wiley-Interscience, New York, 1978).
32. A. E. Glassgold, R. Lucas, A. Omont, *Astron. Astrophys.* **157**, 35 (1986).
33. Truong-Bach, Nguyen-Quang-Rieu, A. Omont, H. Oloffson, L. E. B. Johansson, *ibid.* **176**, 285 (1987).
34. J. R. Heath *et al.*, *J. Am. Chem. Soc.* **109**, 359 (1987).
35. M. E. Geusic *et al.*, in *Metal Clusters*, F. Traeger and G. zu Putlitz, Eds. (Springer-Verlag, Berlin, 1986), pp. 209–217.
36. M. E. Geusic *et al.*, *J. Chem. Phys.* **84**, 2421 (1986).
37. Y. Gu, M. L. Lesiecki, S. E. Bailkowski, W. A. Guillory, *Chem. Phys. Lett.* **92**, 443 (1982).
38. F. J. Kohl and C. A. Stearns, *J. Chem. Phys.* **52**, 6310 (1970).
39. The National Optical Astronomy Observatories are operated by the Association of Universities for Research in Astronomy, Inc., under contract with

Solid-State Ice Volcanism on the Satellites of Uranus

DAVID G. JANKOWSKI AND STEVEN W. SQUYRES

Voyager images of the uranian satellites Ariel and Miranda show flow features with morphologies indicating that ice has been extruded to the satellites' surfaces in the solid state. These images provide the first observational evidence for solid-state ice volcanism in the solar system. Topographic profiles have been measured across a number of flow features on Ariel. With a simple model of extrusion, spreading, and cooling of a viscous flow, the initial viscosity of the flow material is found to have been no more than about 10^{16} poise, far lower than expected for H_2O ice at the ambient surface temperatures in the uranian system. Sharply reduced viscosities may have resulted from incorporation of ices like NH_3 or CH_4 in the uranian satellites.

O NE OF THE MOST INTERESTING results of the Voyager mission to Jupiter, Saturn, and Uranus has been the extent to which even small icy satellites of those planets have undergone geologic resurfacing (1–5). It generally has been uncertain, however, whether the resurfacing has taken place in the liquid or solid state. In the jovian system, buoyancy considerations seem to favor extrusion of warm, mobile ice rather than liquid water (6). However, no landforms clearly indicative of solid-state extrusion have been observed there. On the smaller saturnian satellites, mobility considerations favor extrusion of liquid (7), and the observed morphology is at least consistent with this interpretation. In the uranian system, there is morphologic evidence for extrusion in the solid state (5). In this report we consider this evidence, quantify the morphology of the flows, derive approximate viscosities at the time of extrusion, and consider the implications of these viscosities for the compositions and thermal histories of the uranian satellites.

The morphologic evidence for solid-state resurfacing on the uranian satellites is best developed on Ariel (Figs. 1 and 2). Much of the satellite's surface is transected by a pattern of linear graben-like canyons. On the floors of some of the grabens are deposits that have low crater densities compared to the rest of the satellite (8) and have topographic profiles that appear to be strikingly smooth and convex. They appear to steepen significantly at the margins, in what seem to be flow fronts. Some flows contain medial grooves running parallel to the graben walls. The convex topography and the concentration of the deposits in grabens strongly suggest that these deposits are materials that were extruded to the surface in the solid state, probably in an extensional environment.

In some cases, the flows appear to have been confined by graben walls. In others, however, they clearly have not. Figure 1 shows an instance where the lateral extent of a flow within a canyon remains relatively constant along the canyon's length, whereas the width of the canyon changes from that of the flow to roughly three times it. Figure 2 shows an instance where a flow has spread out across a plains unit, partially burying an impact crater.

It is likely that the sources of most flows were linear fracture systems on the graben floors. This interpretation is supported by (i) the likelihood that extensional fractures associated with grabens would parallel the graben walls; and (ii) the apparent steep flow fronts and limited lateral extent of some flows, indicating that they spread a short distance laterally rather than flowing long distances parallel to the graben walls. In large terrestrial grabens, volcanism is commonly concentrated along vents near the graben axis (9–11); such may also be the case on Ariel. At least some of the medial grooves may be the juncture of two independent flows that have been extruded from parallel fractures on a graben floor, have spread laterally and met, but have not completely coalesced.

Evidence for solid-state resurfacing is also observed on Miranda (Fig. 3). Miranda's surface consists of two types of materials: an old, heavily cratered terrain and a younger terrain transected by a complex pattern of subparallel bands, scarps, and ridges. Areas of this younger terrain are known as "coronae." In some places where corona materials come into contact with the ancient heavily

Center for Radiophysics and Space Research, Cornell University, Ithaca, NY 14853.

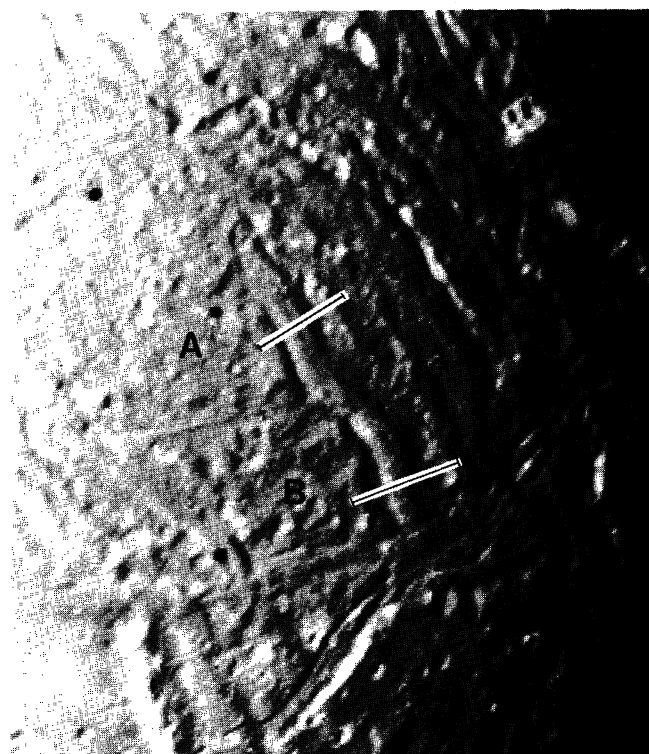**Fig. 1.** Flow region near 30° south, 60° west. Photoclinometric scan lines are marked A and B.